OPTIMIZATION OF THE AFT-BODY GEOMETRY OF AXI-SYMMETRIC SLENDER BODY BASED ON WAVE DRAG CONSIDERATIONS

Harijono Djojodihardjo[1], Eddy Priyono[2] and Lavi R.Zuhal[3]
Department of Aeronautics and Astronautics, Institut Teknologi Bandung
Jalan Ganesya 10, Bandung 40132, Indonesia
harijono@djojodihardjo.com

Key words: Aerodynamics, Computational Fluid Dynamics, Optimization, Slender body, Transonic Flow, Supersonic Flow, Axi-symmetric Flow, Shock-generation

Abstract

The objective of the present work is to establish a comprehensive, universally valid, elegant and yet simple method to design slender axisymmetric body of minimum wave drag in transonic and supersonic flows, taking advantage of the progress of computational aerodynamics and optimization technique. Computational aerodynamics will also be used as a tool for numerical experiments in gaining physical understanding of the drag mechanism due to the geometry of the aft-body, such as the correlation between wave drag and wave distribution of the aft-body geometry, by analyzing previously known optimum aerodynamic shapes as well as verifying the validity of those obtained through minimization scheme. Due to its universality and elegance, the Modified Feasible Direction (MFD) based optimization program will be utilized, along with the linear slender body aerodynamics, also due to its elegance and which could shed some light on the generic optimization scheme. The efforts will be focused on inviscid flow. Based on the physical understanding gained above, a practical method of reducing the wave drag of a given body is developed for both bodies with pointed end and with base area, using shock wave generator at a particular location on the aft body.
Upon validaton of the MFD optimization program by bench-marking the results with the existing optimum axi-symmetric slender bodies, the program is used to search for optimum aft body geometries which minimize the wave drag. The results show that the MFD optimization program can be effectively utilized in an aerodynamic optimization problem.

1. Introduction

The drag minimization of slender axisymmetric body, particularly in the transonic and supersonic flow regimes, has received much interest since it is one of the fundamental problems of aerodynamics. Both theoretical and practical interest leads to the efforts to find the area distributions of slender axi-symmetric bodies, which for a given constraints, such as length, volume, maximum diameter or else, give the minimum possible wave drag. Several geometrical optimization schemes have been utilized for optimum aerodynamic performance. Pioneering effort in the geometrical optimization of bodies of revolution, in particular slender axisymmetric body, for minimum wave drag, has been carried out by von Karman[1], followed by others [2]-[8]. Linearized aerodynamic approach as solution to the wave equation allows the drag to be superposed of conical solutions of an integral over a distribution of sources in supersonic flow, where the sources are equivalent to the local rate of change of the cross-sectional area of the body along its length. Using calculus of variations, minimum-wave-drag bodies for various isoperimetric conditions were determined. Families of bodies of revolution known as von Karman's Ogive [1][2], Sears-Haack Body(Sears [3], Haack [4])., Adams-Haack Body etc are well known slender bodies of revolution of minimum wave drag with various constraints. Later on Ward[5] derived the slender-body approximation for the drag of bodies with a non-zero rate of change of cross-sectional area at the base. Adams[6] considered several minimum-wave-drag problems on the basis of Ward's equation, and arrived at similar minimum-

---

[1] Professor, Universitas Al-Azhar Indonesia and Universiti Sainse Malaysia, formerly Professor, Department of *Aeronautics and Astronautics*, Institute of Technology Bandung
[2] Director for Scientific Research, Defence Research Office and Faculty Member, Nurtanio Institute of Technology and formerly PhD Student, Institute of Technology Bandung,
[3] Lecturer, Department of *Aeronautics and Astronautics*, Institute of Technology Bandung and Universitas Al-Azhar Indonesia

wave drag body as von Karman's, i.e. it has zero slope at the base. Parker [7] presented a linearized-drag integral for bodies of revolution in a double integral form depending explicitly upon the source-distribution function, which is applicable to a larger class of bodies than the usual slender-body, and which reduces to Ward's drag expression in the proper limit, in the supersonic range. Adams [6] and Harder and Rennemann[8] carried out similar analysis on boattail bodies of revolution having minimum wave drag.

With the progress of CFD that has taken place to date, codes are available to look into the detailed flow characteristics and the resulting wave drag, in particular due to the geometry of the aft-body. To the authors' knowledge, a universally valid geometrical design technique for optimum drag of axi-symmetric bodies has not been comprehensively available in the literature and need be further elaborated. Therefore it is the objective of the present work to look carefully into the drag mechanism due to the geometry of the aft-body, since such body has found many applications, also in the light of boattailing and rounding off techniques. The latter may involve shock-boundary layer interaction, which should be taken into account, either a priory or a posteriori, in the optimization of the geometry for minimum total drag. Hence the present study is focused on finding a general optimization scheme, that may give novel results. Although the study is focused on boattail axi-symmetrical bodies, the study of pointed bodies are also carried out to shed some light into the general optimization scheme as well as to understand the detailed characteristics of drag mechanism. Furthermore, the study is devoted into axisymmetric body without lift generation. A preliminary study carried out by the authors[9] to look into the influence of viscosity has confirmed earlier results of Heaslet and Fuller[10] that the viscous contribution to the drag is relatively small in these cases.

Basically, the drag force is divided into two categories, the drag due to skin friction, known as skin friction drag, and drag due to pressure exerted by the fluid to the surface of the object which gives rice to forces acting normal to the boundary surface, known as pressure drag. The pressure drag can be differentiated further into drag due to vorticity released to the flow, and wave drag, which is present only in supersonic flow.

The analytical and computational studies related to the minimization of drag by geometrical considerations will start with inviscid flow, and the effect of viscosity can later on be incorporated. For many engineering purposes it is possible to make useful predictions and design calculation for a steady flight by linearized model and use of the principle of superposition for drag due to viscosity and that occuring in inviscid medium. For supersonic flight, first order analysis for inviscid fluid has been adequate. The perturbation velocity potential of the flow field satisfies the wave equation, and the pressure drag of non-lifting configurations results from the accumulation of energy in the waves induced by the body during its motion.

The analysis for such inviscid flow in the transonic and supersonic regime for axisymmetric flow has been comprehensively treated by Ashley and Landahl [11], using singular perturbation technique and mathematical approximations introduced by Oswatitch and Keune[12]. The drag formulation used for in the optimization search following certain optimization schemes will follow such an approach, due to its powerfulness as an analytical tool.

This method is convenient to reveal the generic contributions of geometrical elements to the drag, and will be useful in understanding the characteristics of several slender axi-symmetric body configurations. Classes of axi-symmetric slender bodies will be identified, including their limitations. Corresponding optimum geometry problem will be defined and formulated through analytical means. Transonic Small Perturbation Method Routine that can also be used for rapid computation to be incorporated in the optimization scheme has also been developed (Djojodihardjo, Widodo et al, [13], and Djojodihardjo & Widodo [14]).

2. Fluid Dynamics Governing Equations

Consistent with our approach to look only into the inviscid flow characteristics, assumptions will be made in the Governing Equations for transonic and supersonic flow, that the flow is steady, irrotational and adiabatic with no energy transfer, no body forces and no shear stresses (inviscid flow).

For the inviscid flow analysis to be incorporated in the optimization scheme, in particular for the drag prediction to be utilized as the Objective Function in the MFD optimization approach, first order slender body aerodynamics as approximation originally formulated by von Karman & Moore (Ashley and Landahl[11], Liepmann and Roshko[15]) will be followed. The drag coefficient for axi-symmetrical slender body can then be expressed as[11][15]:

$$C_{D1} = \frac{[S'(L)]^2}{2\pi} \log\left(\frac{2}{\lambda\sqrt{(L)}}\right) + \frac{1}{\pi}\left[S'(x)\int_0^x S''(\xi)\log(x-\xi)\,d\xi\right]_{x=0}^{L} - \frac{1}{\pi}\int_0^L\int_0^x S''(x)\,S''(\xi)\log(x-\xi)\,d\xi\,dx \quad (2.1)$$

where,

S is the cross sectional area $S(x) = 2\pi R^2$, $S'(x) = 2\pi RR'$ is the first derivative of S(x), $S''(x) = 2\pi(R.R'' + R'.R')$ is the second derivative of S(x) and L = total length of body

Equation (2.1) was first given by von Karman. For bodies with pointed nose and end or ends with the slope of the base equal to zero, equation (2.1) reduces to

$$S(L)C_{D1} = -\frac{1}{\pi}\int_0^L\int_0^x S''(x)\,S''(\xi)\log|x-\xi|\,d\xi\,dx \quad (2.2)$$

Equation (2.2) implies that the drag coefficient of a slender body in supersonic flow using slender body approximation is independent of Mach number.

3. Optimization Approach using Most Feasible Direction (MFD) Method

3.1. Modified Feasible Direction (MFD) optimization

Geometrical optimization using equation (2.1) or (2.2) then give rise to the variational problem that can be treated with standard method, Through such analysis, an optimum shape of a slender body of revolution with pointed nose and has a base area known as the von Karman ogive[1][2] is obtained. Similar variational optimization scheme leads to other minimum wave drag geometries mentioned before[3]-[8].

The present approach is intended to look into finding other optimum slender body of revolution shapes by carrying out optimization scheme which may cover a larger class of bodies, through numerical approach. For that purpose, the Modified Feasible Direction (MFD) method will be followed in the optimization scheme. This method incorporates information about the constraints directly into the optimization problem rather than converting the problem to an equivalent unconstraint one.

Since the objective of the optimization scheme is to find body-of-revolution geometries that have minimum drag in transonic and supersonic inviscid flow, the objective function is defined as the wave drag. For the geometries to be acceptable, a certain set of specified requirements known as constraints should be specified. These constraints can be defined as the length and diameter, maximum cross sectional area and slope of the contour of the body. In addition, the shape of the aft section of axi-symmetric slender body can be assumed to be the function of the design variables and will be the focus of the present work.

The basic concept of Modified Feasible Direction (MFD) optimization can be outlined as follows. Let the wave drag as the objective function F, which should be minimized, be formulated as

$$F \equiv F(\bar{X}) \quad (3.1)$$

a function of the vector of design variables $\bar{X}$, which will be calculated successively following the optimization iteration scheme:

$$\bar{X}^q = \bar{X}^{q-1} + \alpha^*.\bar{S}^q \quad (3.2)$$

where q is the iteration number, S^q is the search direction, and α^* is a scalar multiplier determining the change in $\bar{X}$ for this iteration. The search direction S which leads to the minimization of F should be sought at each iteration scheme to update the $\bar{X}$ vector in the process. The search direction will rapidly reduce the objective function but should be maintained within a feasible design. Following the MFD scheme (Vanderplaats, [16][17]), the general statement of the problem to find the minimum of the Objective function $F(\bar{x})$ subject to inequality constraint as well as side constraints is then given as follows :

Minimize the Wave Drag as the Objective function

$$F(\bar{X}) \quad (3.3)$$

Subject to a set of Inequality Constraint

$$g_j(\bar{X}) \le 0 \qquad j = 1,\ldots,n_g \quad (3.4)$$

a set of Equality Constraint

$$h_k(\bar{X}) = 0 \qquad k = 1,\ldots,n_h \quad (3.5)$$

a set of Side Constraint

$$\bar{X}_i^l \le \bar{X}_i \le \bar{X}_i^u \qquad i = 1,\ldots, n, \quad (3.6)$$

Where $\bar{X} = [x_1, x_2, \ldots\ldots, x_n]$ (3.7)

is the vector of Design Variables.

Equation (3.2) represents a one dimensional search since the update on X^q depends only on the single scalar parameter α, while α* is the value of α that yields the optimal design in the direction defined by S^q. At each iteration step, a new search direction S^{q+1} must be found to reduce the value of the objective function F (i.e."the elevation at the hill") but still satisfies the constraints, i.e. the vector $\vec{S}$ is kept within the usable-feasible direction ("the inside

the constraint fence"). At each step, a usable-feasible direction will be sought, where a usable direction is one that moves downhill while feasible direction is one that keeps the target value inside the fence.
The Kuhn Tucker condition is also utilized to insure that the vector $\vec{X}$ meets the optimum design requirements[16].

3.2 Finding the Search Direction $\bar{S}^q$

The first step in finding the search direction is to determine which constraints, if any, are active or violated. An active constraint is defined as one with values ranging between a small negative number, here designated as CT, and a small positive number, here designated as CTMIN. Typical values for CT and CTMIN are -0.03 and 0.003, respectively. Depending on the values of the constraints compared to CT and CTMIN, the constraints can be differentiated into three categories.
If:

$g_j(x) < CT$, then the constraints are non-active (3.8)

$CT \le g_j(x) \le CTMIN$, then the constraints are active (3.9)

$g_j(x) > CTMIN$, then the constraints are violated (3.10)

Using the active constraint criteria, the algorithm first sorts all the constraints and identifies those that are active or violated. Then the gradients of the objective function and all the active and violated constraints are calculated. Thereafter, a usable-feasible search direction is found (if one exists). In this case, there are three possibilities :

(1) There is neither active nor violated constraints.
(2) There are active constraints but no violated constraints.
(3) There are one or more violated constraints.

3.3 Finding the scalar parameter α*

Having determined a usable-feasible search direction, the next problem is to determine the scalar parameter α* , i.e. the extent of how far the design can be moved in that direction. The basic concept is to try some initial value α* in Equation (3.2) and evaluate the corresponding objective and constraint functions. At the beginning of the iteration process, the values of the objective and constraints are known at lower value $\alpha^* = 0$ and upper value $\alpha^* = \alpha_1$ where α_1 is the initial estimate for α^* given by Vanderplaats [16] :

$$\alpha^*_{est} = \frac{g_j\left(\bar{x}^{q-1}\right)}{\left[\frac{dg_j\left(\bar{x}^{q-1}\right)}{d\alpha^*}\right]} \qquad (3.11)$$

3.4 Convergence Criteria

The optimization scheme carried out through an iterative process requires convergence citeria. There are two kinds of criteria, i.e. relative and absolute criteria. The first criterion requires that the relative change in the objective function between iterations to be less than specified small numerical tolerance. The second criteria is that the absolute change in the objective function between the iterations is less then another specified small numerical tolerance.
Both criteria are used since if the objective function is large, the relative change between two successive iterations is an indication of convergence. If the initial design variables is non-feasible (i.e. the constraints are violated), the first priority is to overcome these violations and find a feasible solution; the absolute change is relevant. The detail of these procedure can be found in ref.[16] and [20].

4. CFD Analysis of Selected Axi-symmetrical Slender Body

4.1.CFD Analysis of Sears-Haack Geometry

In the following example, CFD numerical computation approach is carried out for Sears-Haack geometry. The flow characteristic for inviscid flow condition at Mach number of 1.2 and 3.0. is evaluated.

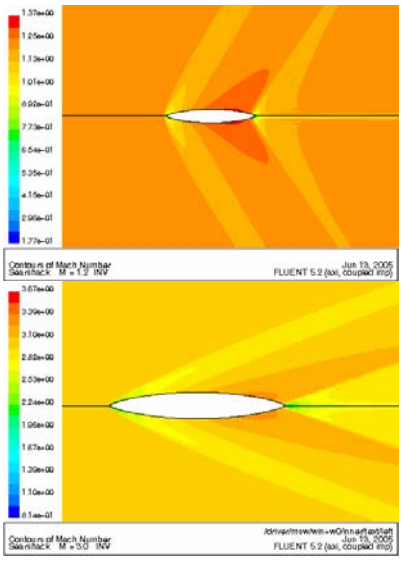

Fig.4.1-a-b Mach Number Contour of Sears-Haack at M = 1.2 and 3.0

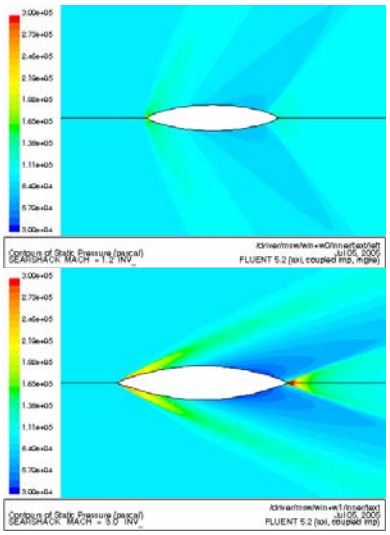

Fig. 4.2-a-b Static Pressure Contour of Sears-Haack at M = 1.2 and 3.0

The Mach number contours indicates that the shock wave angle at the nose as well as at the aft-body tends to be deflected downstream as the Mach number is increased. The location of the shock wave at aft-body also tends to move backward if the Mach number is increased.

As shown in Fig. 4.1-a-b and Figure 4.2-a-b, the attached shocks occurs at the nose and the shock angle depends on the free stream Mach number. As the flow velocity is increased, expansion waves move downstream of the mid section. The shock wave appears again adjacent to the pointed end, accompanied by pressure increase. The downstream pressure for free stream Mach number of 1.2 is lower than the downstream pressure for free stream Mach number of 3.0.

Two methods are utilized to calculate the drag coefficient of the Sears-Haack geometry. The analytical approach using slender body approximation formula given in [11] gives Cd = 0.444. The CFD computation of the drag coefficient of Sears-Haack geometries at M = 1.2 and at M = 3.0 is 0.34037479 and 0.14974916 respectively. The CFD approach is carried out to display the flow field of the Sears-Haack body at Mach numbers of 1.2 and 3.0.

From the discussion of the results, one may conclude that there are shock waves at the aft body region for the axi-symmetric slender body with pointed end. Intuitively, the variation of the distribution of waves on the aft-body will cause the change of the wave drag. Therefore, the study for the modification of the distribution of shock waves is required. This is carried out subsequently as further elaboration of the study reported in ref.[20].

4.2 Sears-Haack Geometry with Shock Generator

CFD analysis of section 4.1. shows that the shallow aft-body generate a weak expansion that is followed by a weak shock. On the contrary, steep aft-body generates a strong expansion and followed by a strong shock that result in a higher wave drag.

In this section, the aft-body wave distribution will be intervened by introducing aft-body shock wave, with the purpose to investigate further the relationship between the aft-body wave distribution and the wave drag. To this end, a shock generator (relatively small flat obstacle) will be placed to force a shock-wave to occur at a specific location. The shock generator is placed at various location at the rear part of the body, and the drag coefficient for the corresponding shock location will be recorded. The Sears-Haack body with shock generator positioned at station 400, 600 and 750 measured from leading edge will be evaluated at Mach number of 1.2.

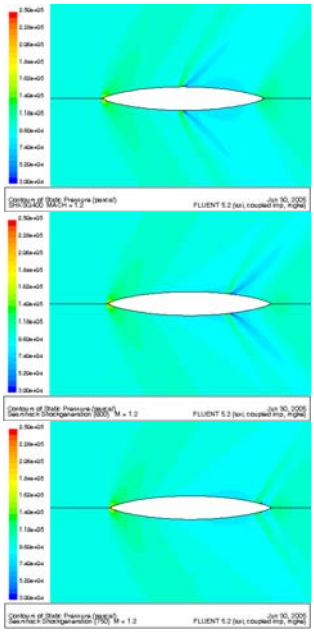

Fig.4.3-a-b-c Static Pressure Contour of Sears-Haack with Shock Generator at x = 400, 600, 750 for Mach = 1.2

The CFD results of Sears-Haack body with Shock Generator are displayed on Fig. 4.3-a-b-c to Fig. 4.5-a-b-c. For a free stream Mach number of 1.2, similar to earlier result without shock generator, there occurs a shock wave at the nose; the local velocity gradually increases along the front surface, but the flow on the aft-body changes due to the presence of the shock generator. The general feature of the flow is characterized by the presence of the shock wave occurring upstream of the shock generator location.

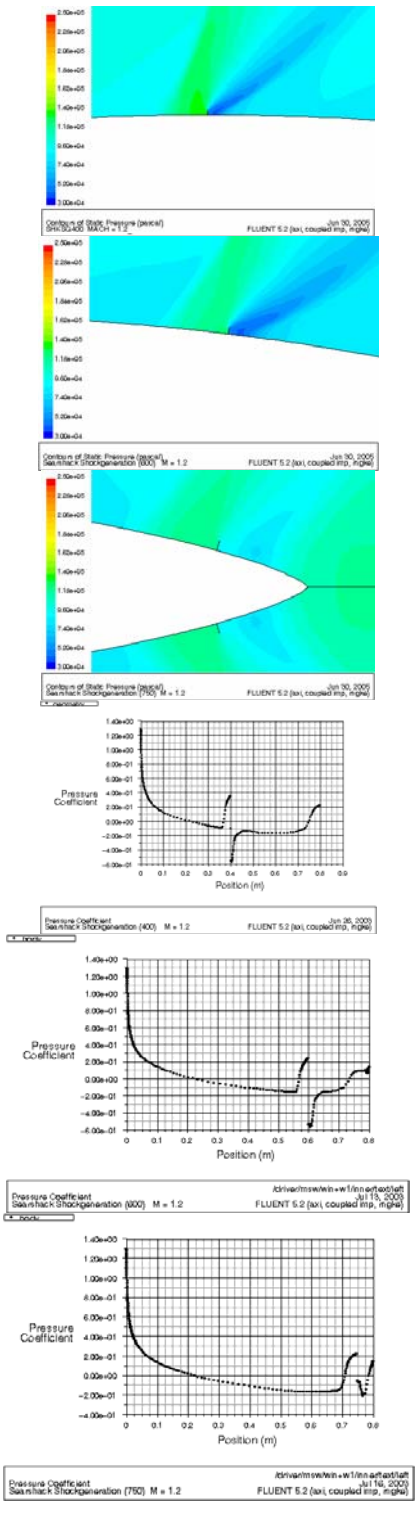

Fig. 4.4-a-b-c Pressure Coefficient of Sears-Haack with Shock Generator at x = 400, 600, 750 for M = 1.2

This is then followed by the expansion wave which occurs downstream of the shock generator. Near the pointed end, another shock is generated. However, this shock is much weaker than the first one.

Table 4.1 summarizes the numerical results obtained for the drag components of the Sears-Haack geometry with various location of shock generator. Among these geometries, Sears-Haack geometry with shock generator at 750 mm (most rearward) seems to give rise to lower drag components.

Table 4.1 Drag Coefficient for Sears-Haack with and Without Shock Generator at Mach = 1.2

No	Geometry	Drag Coeff.
1	SearsHaack without SG	0.34037479
2	SearsHaack with SG at 400	0.29200521
3	SearsHaack with SG at 600	0.26400607
4	SearsHaack with SG at 750	0.21099250

This results indicates that for a given body, especially slender body with pointed end, the drag coefficient can be modified by altering the aft-body wave distribution that results in a lower drag.

4.3 MBB Experimental Bodies

MBB (Messerschmitt Bolkow Blohm) has carried out experiments to evaluate drag of a family of slender bodies of revolution as reported by Lorenz-Meyer and Aulehla [18]. MBB geometry shown in Fig.4.5 is an axi-symmetric slender body created by MBB, consisting of two parts, fore-body and aft-body, with the total length of 800 mm and max diameter of 120 mm. The specific location the starting point of the aft-body is predetermined. The fore-body is characterized by power series, as elaborated in [20]:

$Y_f = a_f .x^3 + b_f .x^2 + c_f .x$ (4.1)

Where : $a_f = y_{max}./x_1^3$, $b_f = - 3.y_{max}/x_1^2$ and $c_f = 3.y_{max}/x_1$

The aft-body geometry characterized by the power series : $Y_h = a_h.x^3 + b_h .x^2 + c_h .x + d$ (4.2)

where :

$a_h = y_{max}/(x_2 - x_3)^3$

$b_h = - 3x_2. y_{max}/(x_2 - x_3)^3$

$c_h = 3x_2^2 . y_{max}/(x_2 - x_3)^3$

$d = (x_3. y_{max}/(x_2 - x_3)^3).(3x_2.x_3 - x_3^2 - 3x_2^2)$

y_{max} = maximum radius = 60 mm

x_1 = midpoint of body = 400 mm

x_2 = starting curve measured from leading edge

x_3 = total length of body = 800 mm

In this work three types of the MBB geometries will be reevaluated by utilizing the CFD approach, and carried out at the transonic flow (Mach = 1.2) and

supersonic flow (Mach = 3.0). The CFD numerical approach is carried out on the MBB geometries in order to obtain their physical flow characteristic indicative as flow over an axi-symmetric slender body with pointed end.

By determining the starting point of the aft-body geometry several MBB bodies can be developed. The CFD investigation is carried out for three MBB geometries namely MBB1 (MBB geometry with the starting point of the aft-body at midpoint), MBB3 (MBB geometry with the starting point of the aft-body at 0.6875 length of body) , MBB5 (MBB geometry with starting geometry at 0.8125 length of body) at Mach = 1.2 and Mach = 3.0. in inviscid flow.

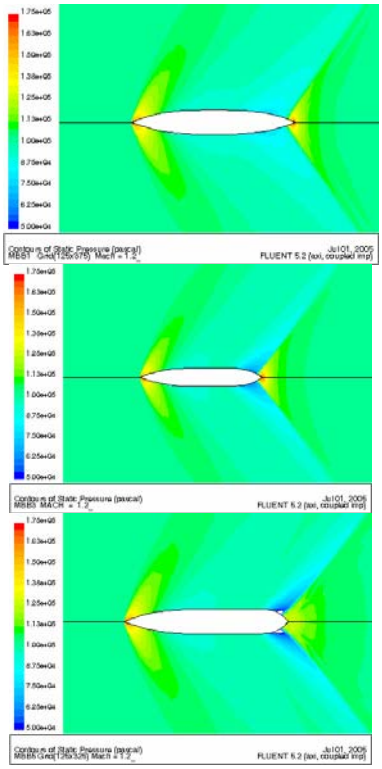

Fig.4.5-a-b-c Static Pressure Contour of MBB-1,MBB-3, MBB-5 at M = 1.2

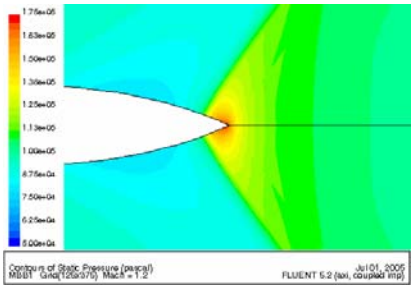

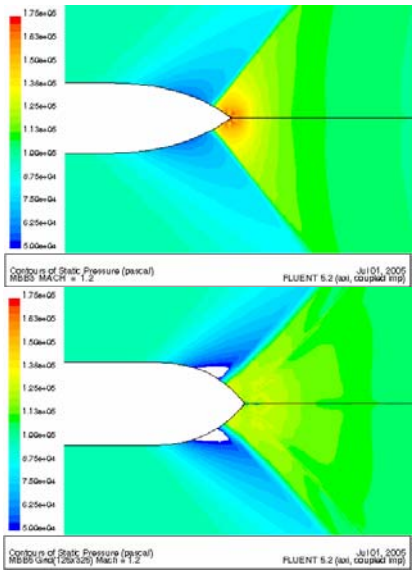

Fig. 4.6 a-b-c Static Press Contour of MBB1, MBB3 and MBB5 Aft-body at Mach = 1.2

The following table summarizes the CFD numerical results obtained for the drag components of the axi-symmetric slender body with pointed end for three geometries with different aft-body. The MBB-1 geometry seems to give the lowest wave drag components compare to the others, as shown in Table 4.2

Table 4.2 Drag Coefficient of MBB Experiment Body

No	GEOMETRY	Drag Coefficient	
		M = 1.2	M = 3.0
1.	MBB-1	0.26769474	0.18607837
2.	MBB-3	0.37780611	0.21508539
3.	MBB-5	0.43300818	0.23530491

CFD results of the MBB experimental geometry reveals several features. The MBB geometry with steep aft-body has a higher wave drag than the others. The MBB geometry with shallow aft-body has relatively lower wave drag. There should be an optimum gradient of the aft-body, which gives minimum wave drag. The next section is devoted to address this notion, i.e to find the optimum MBB geometry by using the MFD numerical approach.

5 Application of MFD Optimization for Wave Drag Minimization of Slender Body

The conservative method to obtain the optimum geometry of axi-symmetric body having minimum drag in the transonic as well as supersonic flow regime can be carried out using traditional iteration process. The iteration process needs more time to

arrive at the optimum result depending on the complexities of the problem. Furthermore the traditional iteration process does not guarantee that a global optimum is achieved. The MFD optimization is a structured numerical optimization, so that it can be applied to minimize wave drag of any axi-symmetric slender body. The structure of the optimization consists of an objective function, equality/inequality constraints as well as side constraints, and the design variables. In this work, the objective function for solving the optimization of axi-symmetrical slender body is the wave drag equation (2.1).

The objective function C_D is expressed in terms of S"(x), and S"(x) and should further be expressed in term of the design variables. The number of the design variables depends on the complexity of the problem. The constraints can be defined depending on the design goal; for example, the geometry of interest can be differentiated into two parts: the fore body, which is an arbitrarily chosen existing geometry, and the aft-body, which is created following any arbitrary function f(x)). The constraints depend on the design parameters such as maximum diameter, length of body and location of maximum cross sectional area. The constraints should be expressed in terms of the design variables, and the number of the constraints depends on the problem at hand.
The MFD optimization codes will be validated using the corresponding constraints of the existing axi-symmetric slender body with pointed end as well as with base area (Sears-Haack and Von Karman). Here the MFD optimization code is developed and utilized to obtain the minimum wave drag of an axi-symmetric slender body. Furthermore, this MFD optimization codes can be applied to a general optimization problem as long as the objective function as well as the constraints are suitably defined.

5.1 MFD Optimization Approach of Sears-Haack Geometry

In this section, the MFD optimization code will be validated. The MFD optimization code which has been developed is verified by evaluating a set of constraints that are consistent with the existing Sears-Haack geometry. The optimum wave drag results are compared to the analytical ones.

The critical parts of the evaluation of the geometry using the MFD optimization approach are the definition of the objective function, the constraints and the design variables. Firstly, the objective function of axi-symmetrical slender body with pointed ends will be determined. The objective function represents the wave drag which is given by the Equation (2.2).
The value of S"(x) can be obtained from the second derivative of S(x), where S(x) is the cross sectional area distribution of the geometry of interest. In this case the cross sectional area S(x) is by the following Equation (see reference [3]) with n = 2. Following the procedure elaborated in section 3, MFD optimization code is developed. For validation purposes, the code is applied for the optimization scheme of well known geometries, and in this particular example, the problem defined for Sears-Haack body. Here, the set of constraints should correspond to the Sears-Haack body. Their optimum wave drag results will be compared.
The objective function is then defined as the wave drag, which for Sears-Haack body is expressed as

$$C_{D1} = -\frac{1}{\pi S(L)} \int_0^L \int_0^x S''(x)\ S''(\xi)\ \log|x-\xi|\ d\xi\ dx \quad (5.1)$$

For convenience, instead of the linear variable of the axial coordinate, angular variable θ is used and defined as:

$$\theta = \cos^{-1}\left(2\frac{x}{L}-1\right) \quad \text{or} \quad x = \frac{L}{2}(1+\cos\theta) \quad (5.2)$$

with θ = 0 at the tail and θ = π at the nose.

The cross-sectional area distribution along the length of Sears-Haack body is given by [3]

$$S(\theta) = \frac{l^2}{4}\left\{X(1)\left(\pi-\theta+\frac{\sin 2\theta}{2}\right)+X(2)\left[\frac{\sin(3\theta)}{3}-\frac{\sin(\theta)}{1}\right]\right\} \quad (5.3)$$

Table 5.1 Result of MFD optimization Approach of Sears-Haack

No	Initial Design Var		*Optimum Design Variables*		*Objective*Function F(x)
	X1	X2	X1	X2	
1.	0.1	0.1	0	-0.0942	0.3567
2.	0.5	0.5	0	-0.0941	0.3564
3.	1.0	1.0	0	-0.0942	0.3564
4.	1.2	1.2	0	-0.0942	0.3564
5.	2.0	2.0	0	-0.0942	0.3566

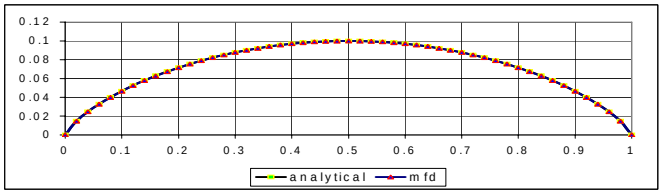

Fig.5.1. Sears Haack Geometry obtained using Analytical and MFD Optimization Approach

where X(1) and X(2) corresponds to A_1 and A_2, respectively, and are chosen to be the design variables. The length L, the maximum cross-sectional area (πr_{max}^2)and its position along the length of the body are defined. Then two sets of constraints can be defined, these are S(0) = 0 and $S(\pi/2)= \pi r_{max}^2$. Going through the algebra, the following constraints are defined:

1. $g(1) = S(0) = \frac{x_{max}^2}{4} X(1).\pi$ (5.4) and

2. $g(2) = \frac{x_{max}^2}{4}\left(X(1)\frac{\pi}{2} - 1.3333\ X(2)\right) - \pi r_{max}^2$ (5.5)

The results of the MFD optimization code with several values of initial design variables corresponding to the maximum radius R_{max} = 0.1 and maximum length $L=X_{max}$ = 1.0 is exhibited in Table 5.1

The result of MFD optimization approach gives the constants A_1 = 0 , A_2 = -0.0942 and the Drag Coefficient, C_D = 0.3564. Substituting A_1 = 0 and A_2 = -0.0942 into Equation (5.1) gives the equation of cross sectional area distribution,

$$S(\theta) = \frac{l^2}{4}\left\{-0.0942\left[\frac{\sin(3\theta)}{3} - \frac{\sin(\theta)}{1}\right]\right\} \quad (5.4)$$

The result is plotted in Fig. 5.1 where it is compared with the Sears-Haack area distribution. The MFD output reproduces closely the Sears-Haack area distribution. Hence, MFD output of the problem, with set of constraints consistent with Sears-Haack geometry, gives the Sears-Haack area distribution. Therefore, the MFD optimization code has been validated.

5.2 MFD Optimization of MBB Geometry

The MFD optimization program validated in the previous subsection is applied for finding the MBB geometry which has a minimum wave drag. The optimization problem of the objective function objective function of this investigation is Equation (5.1). The value of S"(x) can be determined from the geometrical properties of the candidate optimum geometry. An example is depicted in Fig. 5.2. The

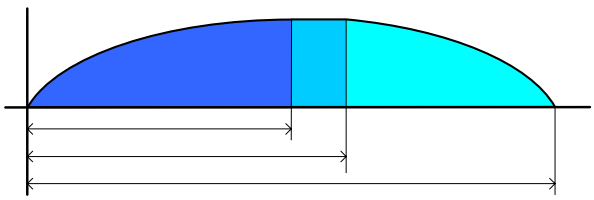

Fig. 5.2. Case Study Geometry with Pointed Ends

geometry considered consists of two parts namely the fore-body (Curve O-A) and aft-body (Curve B-C), connected by a cylindrical section (A-B).

The fixed fore-body (Curve O-A) is adopted from the MBB geometry.

$f_1(x) \approx R(x) = a_f .x^3 + b_f .x^2 + c_f .x$ (5.5)

where :

$a_f = R_{max}./x_1^3 = 0.1/0.5^3 = 0.8$

$b_f = -3.R_{max}/x_1^2 = -3 \times 0.1/0.5^2 = -1.2$

$c_f = 3.R_{max}/x_1 = 3 \times 0.1/0.5 = 0.6$

Here, R_{max} = 0.1 and x_1 = 0.5.

Then the equation of the fore-body is $R(x) = 0.8 X^3 - 1.2 X^2 + 0.6 X$

The mid-section is a cylinder with radius r_{max}, (A-B), and starts at X = 0.5 to X_{SC} (starting point of aft-body curve). In this case, X_{SC} is varied from 0.5 to 1.0, and this point is designated as the design variable. The equation of mid-section is

$f_2(x) \approx R(x) = rmax$ (5.6)

The aft-body (Curve B-C) is formulated as a polynomial of order 3, with origin at point B(X_{SC}, r_{max}) and end at point C(x_{max}, 0) , maximum radius = 0.1 and intersects the X axis at x_{max} = 1.0. The aft-body curve $f_3(x)$ can be expressed as :

$R(x) = a .x^3 + b .x^2 + c .x + d$ (5.7)

where the curve $f_3(x)$ passes through point B(X_{SC}, rmax) and point C(x_{max}, 0) and the slope of $f_3(x)$ at point B(X_{SC}, r_{max}) is equal zero. Then the coefficients a, b, c and d should be expressed in term of the known values (rmax and xmax) and the design variable (X_{SC}).

$R_{max} = a. X_{SC}^3 + b. X_{SC}^2 + c. X_{SC} + d$ (5.8)

The curve $f_3(x)$ passes through the point C(xmax, 0) then:

$0 = a. xmax^3 + b. xmax^2 + c. xmax + d$ (5.9)

$Rmax = a (X_{SC}^3 - xmax^3) + b (X_{SC}^2 - xmax^2) + c(X_{SC} - xmax)$

The slope of $f_3(x)$ at point B(X_{SC}, rmax) is equal to zero

$R' = 3a X_{SC}^2 + 2b X_{SC}^2 + c = 0$ (5.10)

By evaluating Equation (5.8)-(5.10) the constraints a, b, c and in term X_{SC}, Rmax and xmax can be obtained :

$$a = \frac{R\max}{(X_{sc} - x\max)^3}$$

$$b = \frac{-3 X_{SC} R\max}{(X_{SC} - x\max)^3}$$

$$c = \frac{3 X_{SC}^2 R\max}{(X_{SC} - x\max)^3}$$

$$d = \left(\frac{x\max . R\max}{(X_{SC} - x\max)^3} \right) . \left(3.X_{SC}\, x\max - x\max^2 - 3.X_{SC}^2 \right)$$

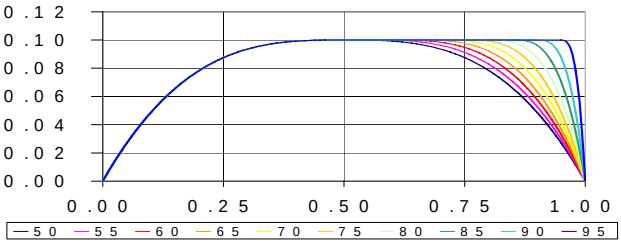

Fig. 5.3 Optimum Geometry Possibilities

The optimization procedure is feasible when the constraints are satisfied. In this case the constraints are determined from the possible values of the starting point coordinate X_{SC} , where $0.5 \leq X_{SC} \leq 1.0$. Fig. 5.3 shows the possible geometries obtained by varying the value of X_{SC}.
Hence in this problem the constraints in term of design variable X_{SC} can be written as :

$$g(1) = 0.5 - X_{SC} \qquad (5.11)$$

$$g(2) = X_{SC} - 1.0 \qquad (5.12)$$

The output of the MFD optimization program with the initial design variable $X_{SC} = 0.1$ is shown in Table 5.2.

Fig.5.4 successive geometries as the result of the MFD iteration process

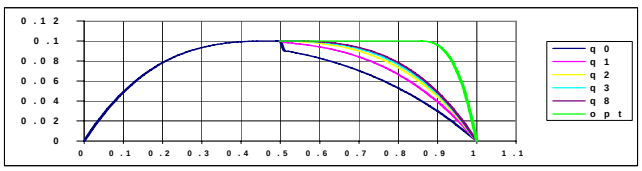

Figure 5.4 plots the successive geometries resulting from the MFD iteration process. The optimum geometry of the axi-symmetrical slender body with pointed ends is depicted in Fig. 5.5.

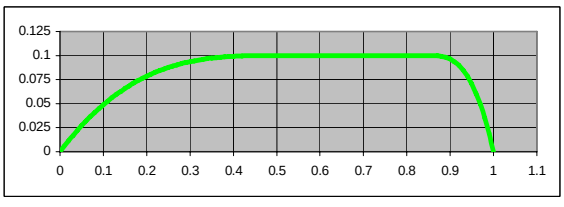

Fig. 5.5 Optimum Geometry of MBB-like body

The MFD optimization program gives the optimum drag of Cd = 0.3592484 which is satisfied by a geometry with X_{SC} at 0.85.

5.3. CFD Validation of Optimum MFD Geometry

In this section, CFD computational study is carried out to validate of the optimum MBB geometry, which is a family of axi-symmetrical slender bodies with pointed ends, and to look into the flow characteristics and to investigate the significant elements that contribute to the wave drag.

Based on the result of the MFD optimization approach, the optimum value of MBB geometry with pointed ends is the geometry with $X_{SC} = 0.85$. The investigation is not only concerned with the search for the optimum geometry, but also to look into the effect of the variation of the position of the X_{SC} point, at which the aft-body curve coincided with the cylindrical mid-section.
These geometries are also represented by using the polynomial order three ($f_3x = a.x^3 + b.x^2 + c.x + d$). For convenience, three geometries are considered:
Body A with aft-body curve starting at 0.75, with aft-body curve represented by $f_3x = -6.4\ x^3 + 14.4x^2 - 10.8x + 2$. (upstream of optimum geometry).

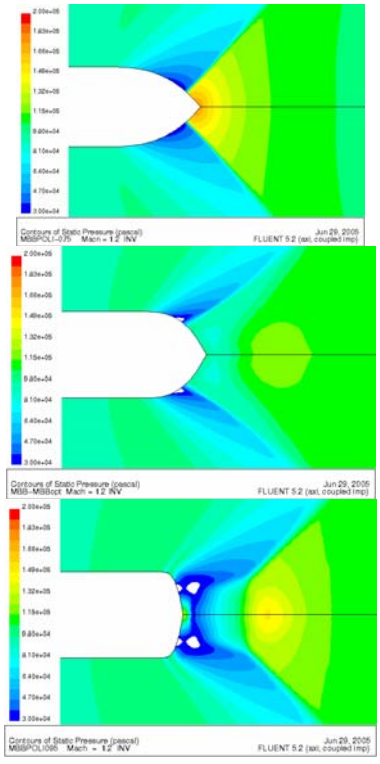

Fig. 5.6-a-b-c Static Pressure Contour of Case Study Geometry (Aft-body Section, Body A, Body B and Body C) at Mach = 1.2

Body B with aft-body curve starting at 0.85, with aft-body curve represented by f $f_3x = -29.63\ x^3 + 75.56x^2 - 64.22x + 18.30$ (optimum geometry).

Body C with aft-body curve starting at 0.95, with aft-body curve represented by $f_3x = - 800x^3 + 2280x^2 - 2166x + 686$. (downstream of optimum geometry).

Rampant/Fluent Flow Solver [21] is utilized to explore the aerodynamic characteristics, especially the wave drag, by applying the free stream Mach number of 1.2 and 3.0. The results are exhibited in Fig. 5.6-a-b-c. It can be seen in that the base of Body B has larger region of lower pressure compared to Body A and C. Therefore the Body B has a lower drag compared to Body A and Body B.

Table 5.2. Contribution of Slender Body Sections to the Drag Coefficient (Cd) of Case Study Geometry with Pointed End

Mach number	Body Section	CASE STUDY		
		BODY A	BODY B	BODY C
1.2	fore	1.17475	1.17481	1.17541
	mid	-3.8759e-09	5.8961e-06	-3.9499e-08
	aft	-0.607594	-0.700233	-0.587099
	total	0.5671576	0.4745911	0.5883180
3.0	fore	0.337934	0.3381056	0.3379349
	mid	-1.7968e-09	2.9711e-09	4.1853e-07
	aft	-0.0310517	-0.050358	-0.047258
	total	0.3068830	0.2877474	0.2906767

6 Optimization of Axi-symmetric Slender Body with Base Area

This section will explore several selected axi-symmetric slender bodies with base area. The study includes existing well-known geometry (Von Karman, Haack-Adams and slender body with different aft-body), and then followed by case-study axi-symmetric slender bodies with base area. The three geometries (Von Karman, Haack-Adams and Case study geometry) were build with the same diameter and length, which are 100 mm and 1000 mm, respectively. The wave drag of both the existing geometry and the case study geometry will be evaluated by using equation (2.1). .Three methods of approaches, i.e. Analytical, MFD Optimization and CFD Approach, will be applied to both existing and the case study geometries. The CFD approach is intended also to look whether the candidate case study geometry has favorable (optimum) wave drag characteristics.

6.1 Analytical and CFD Approach for Existing Geometry

CFD Analysis of Von Karman Geometry

The flow characteristics of von Karman geometry will be studied. The CFD numerical approach is applied to von Karman geometry at Mach numbers 1.2 and 3.0 for inviscid flow condition.

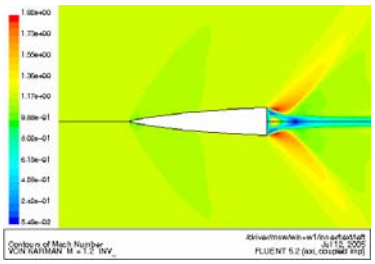

Fig.6.1-a Mach Contour for Von Karman Geometry Mach = 1.2

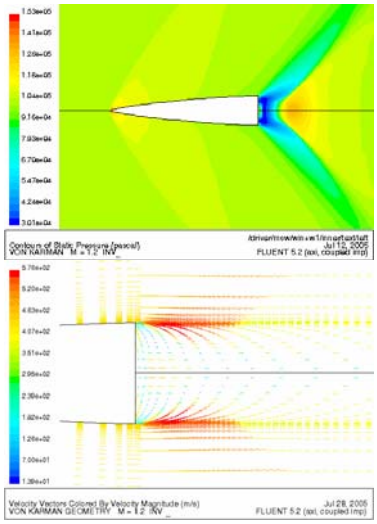

Fig. 6.1-b -c Static Pressure Contour and Velocity Vector for Von Karman Geometry at Mach = 1.2

The result of CFD analysis is shown at Fig. 6.1-a, and Fig. 6.1-b-c. It can be seen that the shock wave angle at the nose as well as at the aft-body tends to deflect downstream with the increase of the Mach number. Expansion waves occur at the edge of the base area, then followed by a shock wave downstream of the base area. Such distribution of waves obviously results in the appearance of a very low pressure region on the base area, which contributes significantly to the overall drag of the body.

The analytical approach for the wave drag, which is independent of Mach number as given in Ref [11], gives Cd = 0.40. The CFD result for M = 1.2 and at M = 3.0 is Cd = 0.47110016 and Cd = 0.17504237, respectively.

Haack-Adams Geometry

Haack-Adams Geometry is an axi-symmetrical slender body with pointed nose and base area. There are three specific families of the bodies. The first family consisting of bodies having a fixed length, given base area, and given maximum area. The second family consists of bodies having a given length, base area and a contour passing through a prescribed point between the nose and base. The third family consists of bodies having given length, volume and base area. Here only the first family will be evaluated.

Analytical Approach to Haack-Adams Geometry

For a given length, base area and maximum area, the area distribution of Haack-Adams Geometry is[6] :

$$S(x) = \frac{B}{\pi c}\sqrt{1-x^2} + \frac{B}{\pi c}\frac{(x-c)^2}{\sqrt{1-c^2}}\ln(N) + \frac{B}{\pi}Cos^{-1}(-x) \quad (6.1)$$

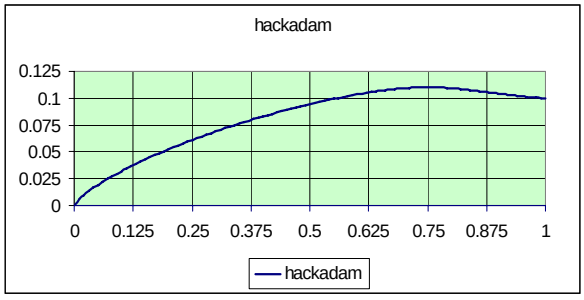

Fig. 6.2 Hack-Adam body with given base radius = .1 , length = 1 and c = 0.25

$$N = \frac{1-c\,x-\sqrt{1-c^2}\,\sqrt{1-x^2}}{|x-c|} \quad (6.2)$$

Where S(x) = cross sectional area distribution
A = max cross sectional of body divided by $(l/2)^2$
B = body base area divided by $(l/2)^2$
c = distance, divided by $(l/2)^2$, from midpoint of body to location of A max.
The relationship between A,B and c is given by,

$$\frac{\pi A}{B} = \frac{\sqrt{1-c^2}}{c} + Cos^{-1}(-c) \quad (6.3)$$

Ref[6] gives the analytical expression for the drag coefficient :

$$C_D = \frac{1}{\pi}\frac{B^2}{Ac^2} \quad (6.4)$$

In the case considered, the maximum length Xmax = 1.0, the base radius rmax = 0.1, and the base area $B = \pi\, r_{max}^2/(l/2) = \pi\, 0.1^2/(0.5)^2 = 0.12566$.
The distance of the point of maximum area to the mid point is 0.25; this gives the value of c = 0.25/(l/2) = 0.25/0.5 = 0.5, π A/B = 3.8264, A = 0.15306
Substituting A, B and c into Equation (6.10) will give the analytical drag coefficient : C_D = 0.13135.
The graph of the first family of the Haack-Adams geometry with given length, base area and the maximum area are depicted in Fig. 6..3.

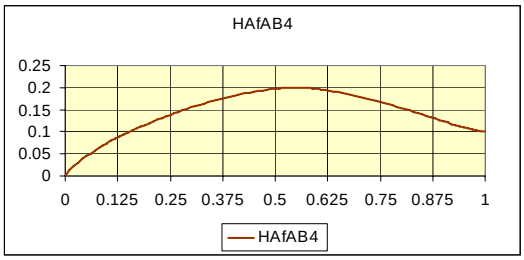

Fig. 6.3 Hack-Adam given length = 1 , base radius = 0.1 and ratio of maximum area to base area f = 4 (Location of max area at 0.55)

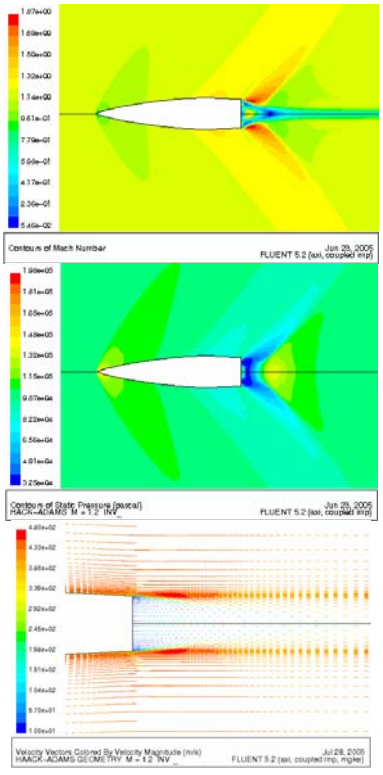

Fig. 6.4-a-b-c Mach Number Contour, Static Pressure Contour and Velocity Vector of Haack-Adams Geometry for Mach = 1.2

CFD Analysis of Haack-Adams Geometry

CFD numerical computation approach is applied to Haack-Adams geometry, for inviscid flow condition at Mach number = 1.2 and Mach number = 3.0..

The result of CFD analysis is depicted at Fig. 6.4-a-b-c. The Mach number contours indicate that the shock wave angle at the nose as well as the aft-body tends to be deflected to downstream with the increase of the Mach number. Expansion waves occur at the edge of the base area, and followed by shock wave downstream of the base area. The aft-body flow looks very similar to that of Von Karman geometry. Slender body drag formula [11] gives predicts Cd = 0.13135, while the CFD results for this geometry, for M = 1.2 and M = 3.0, gives Cd values of 0.5110229 and 0.2277281, respectively.

CFD Calculation of Slender Body with Flat, Rounded and Conical Aft-body

As further development of the work reported in [9], the flow characteristics of slender body with three different aft-body geometries are investigated; these are the flat edge, conical and rounded edge aft-bodies. The calculation is carried out for values of free-stream Mach numbers of 1.2 and 3.0; the angle of attack $\alpha = 0$. For this analysis, all axi-symmetric slender bodies considered (flat base, conical and rounded aft-body geometry) has the same maximum diameter = 12.7 mm and maximum length = 60 mm.

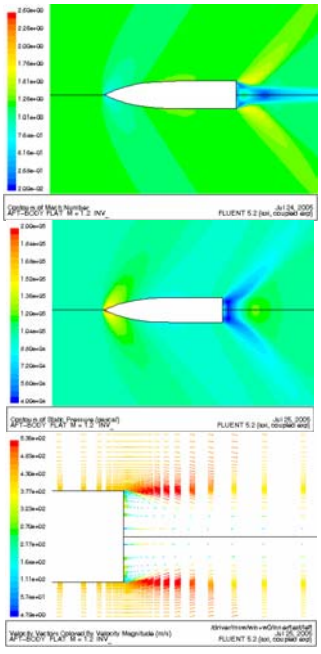

Fig. 6.5-a-b-c Mach Contour, Static Pressure Contour and Velocity Vector of Flat Aft-Body at M = 1.2

The Mach contour and pressure distribution of the axi-symmetric slender body with flat aft-body geometry under study are shown in Fig. 6.5-a-b-c for Mach number =1.2.

In particular, for free stream Mach number M = 1.2 , shocks occur at the bow and at the stern of the axi-symmetric slender body. The presence of shock waves is accompanied by the presence of mach lines that are inclined downstream. The pressure distribution indicates a maximum at the bow of the axi-symmetric slender body, i.e the stagnation point, as expected, and decays towards downstream. At the corner, the pressure decreases sharply. It should be noted, however, that at the aft-body region, the inviscid computational approach may not be valid without proper modeling of the flow. The results thus far obtained may be indicative of the real situation only at the upstream part, especially if there are shocks in the vicinity of the corner.

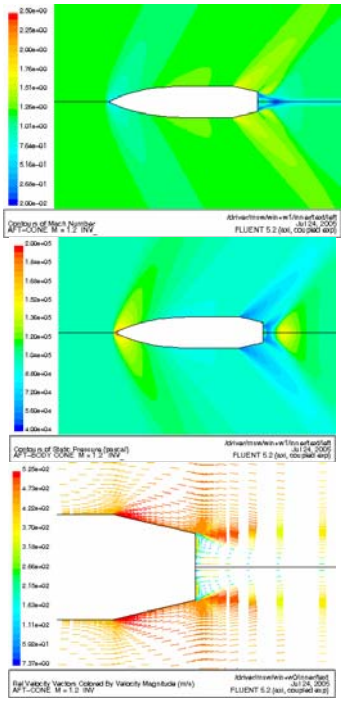

Fig. 6.6-a-b-c Mach , Static Pressure Contour and Velocity Vector of Conical Aft-Body at M = 1.2

The Mach contour and pressure distribution of the axi-symmetric slender body with conical aft-body geometry under study are shown in Figure 6.6-a-b-c for Mach number = 1.2 and for Mach number = 3.0 . For this configuration, at free-stream Mach number M = 1.2 and 3.0, the local velocity is gradually accelerated downstream along the surface until near the stern. The shock waves appear at the front and rear part. Compared to the former geometry, the pressure drops near the beginning of the conical part of the aft-body due to expansion waves. For M = 1.2

and 3.0, the expansion waves also occur near the beginning of the conical part. Wake is shed near the base and strong shock wave appears downstream the body.

The Mach contour and pressure distribution of the axi-symmetric slender body with rounded aft-body geometry under study are shown in Fig. 6.7-a-b-c and for Mach number = 3.0 .
For this configuration, at free-stream Mach number M = 1.2, the local velocity is also gradually accelerated downstream along the surface until near the stern. For M = 1.2, shock waves appear at the front and rear part. Expansion wave occurs near the stern, as indicated also by a sharp pressure jump there.

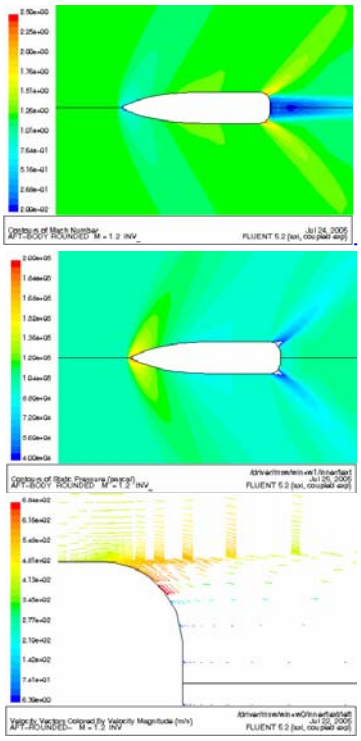

Figure 6.7-a-b-c Mach , Static Pressure Contour and Velocity Vector of Rounded Aft-Body at M = 1.2

The pressure jump occurs at the rounded part of the stern. Comparing the pressure jump here for this geometry with that for the other geometries studied, the pressure jump here is relatively larger.
The following table summarizes the numerical results obtained for the drag components of the axi-symmetric slender body for three different geometry studies. For the drag coefficient calculation, the CFD numerical approach is conducted base on reference value of area = 0.00050675 m^2 (maximum cross sectional area) and reference of length = 0.06 m (maximum length).

Table 6.1 Drag Coefficient of CFD results for Various Aft-Body

No.	AFT-Body	Mach = 1.2	Mach = 3.0
1.	Flat	0.12222553	0.081524489
2.	Cone	0.10648763	0.063160879
3.	Rounded	0.15347332	0.080476319

This particular result indicates that the slender body with the cone aft-body has minimum drag compared to the other two configurations.

6.3 MFD Optimization Approach

Analogous to the MFD optimization of Sears-Haack body, MFD optimization of von Karman ogive is carried out. The result is plotted in Figure 6.8 where comparison is made between von Karman ogive original cross-sectional area distribution with that obtained using MFD optimization. The MFD output resembles von Karman ogive area distribution very closely, which serves to further validate the MFD code developed.

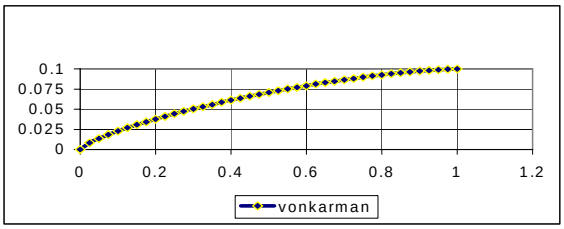

Fig. 6.8 Von Karman Geometry

Optimization of Aft-Body Geometry

The MFD program is next applied to find a geometry that has a minimum wave drag starting from a simple case study geometry. This case study geometry consists of three parts, the fore-body and aft-body, connected by its mid-section, as depicted in Fig.6.9. The fore- body is an arbitrary existing axi-symmetrical slender body, whereas the aft-body will be evaluated later on. The aft-body geometry of interest is represented by a function of F(x) (in this work using a third order polynomial as an example) and the MFD program will be used to find the coefficient of the polynomial which leads to a minimum drag.
In this case, the case study geometry is axi-symmetric slender body with base area, which has a normalized dimension of maximum length = 1 and maximum radius = 0.1.

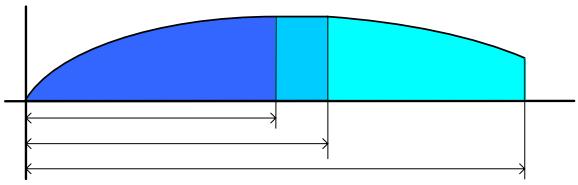

Fig. 6.9 Case Study Geometry with Base Area

The fixed fore body (Curve O-A) is adopted from the MBB geometry previously discussed.

The mid section is cylindrical with a radius of r_{max}, (A-B) starts at X = 0.5 and ends at X_{SC}. Point X_{SC} is varied from 0.5 to 1.0, and is designated as the design variable. The aft-body (Curve B-C) is formulated as a third-order polynomial, starting at point B(X_{SC}, rmax) and ending at point C(x_{max}, 0.5 r_{max}); the maximum radius is 0.1 and the base radius is 0.5 r_{max}.

The aft body curve $f_3(x)$ can be expressed as

$$R(x) = a(X - X_{SC})^3 + b(X-X_{SC})^2 + c(X-X_{SC}) + d \quad (6.5)$$

where the curve $f_3(x)$ passing through point B(X_{SC}, r_{max}) and point C(x_{max}, 0.5 r_{max}) and the slope of $f_3(x)$ at point B(X_{SC}, rmax) is equal zero. Then the coefficients a, b, c and d should be expressed in term of the known value (r_{max} and x_{max}) and the design variable (X_{SC}).

The optimization procedure is feasible when the constraints are satisfied. In this case the constraints are determined by the possible values of X_{SC} point with defined range of $0.5 \leq X_{SC} \leq 1.0$. Going through the algebra [20], in terms of design variable X(1) and X(2) the constraints can be written as :

$g(1) = X(2)$ (IV.18)

$g(2) = 0.5 - X(1)$ (IV.19)

$g(3) = X(1) - 1.0$ (IV.20)

where $X(1) = X_{SC}$ and X(2) = b . MFD optimization program is then applied to obtain the optimum geometry for minimum wave drag.

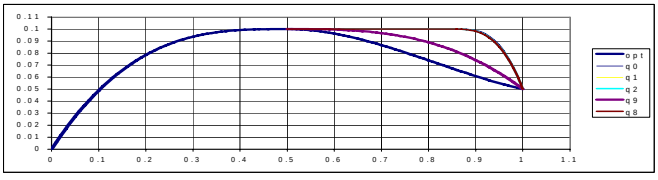

Fig. 6.10 Case Study With Initial Condition X(1) = 0.85 & X(2) = 0.5

Fig. 6.10 plots the corresponding aft-body curves obtained successively from the initial design variables of X(1) = 0.85 and X(2) = 0.5.

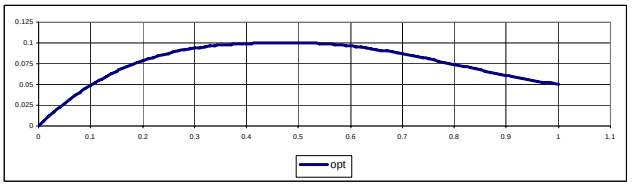

Fig. 6.11 Optimum Case Study Geometry with Base Area

The optimum geometry of axisymmetrical slender body with base areas is depicted in Fig. 6.11. The output of MFD optimization program gives the optimum geometry with X_{SC} = 0.5 , polynomial coefficient of aft-body a = 0.4482, b = 0.4241, c = 0.0 and d = 0.1. The equation of optimum aft-body can be expressed as $R(x) = 0.4482x^3 - 0.4241x + 0.1$. The MFD result gives the minimum drag coefficient for M = 1.2 Cd = 0.4069 , and for M = 3.0 Cd = 0.4013

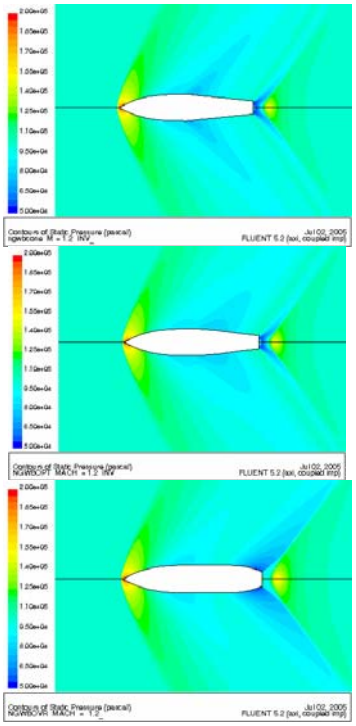

Fig. 6.13-a-b-c Static Pressure Contour of Case Study Geometry Body A, Body B and Body C for Mach = 1.2

CFD Validation for Optimum Case Study Geometry

Three different geometries are considered. For convenience, the following label will be used to identify the three geometries considered,

(1) Body A is case study geometry with aft-body consists of cone start at point A(0.5,rmax) and

C(1.0, 0.05) with the equation of R(x) = - 0.1x + 0.15.

(2) Body B is case study geometry with starting point of curve at X_{SC} = X(1) = 0.5 and the polynomial of aft-body is R(x) = $0.4482x^3$ – 0.4241x + 0.1.

(3) Body C is case study geometry with starting point of curve at X_{SC} = X(1) = 0.6994 and the coefficient of polynomial b = X(2) = 0.0.

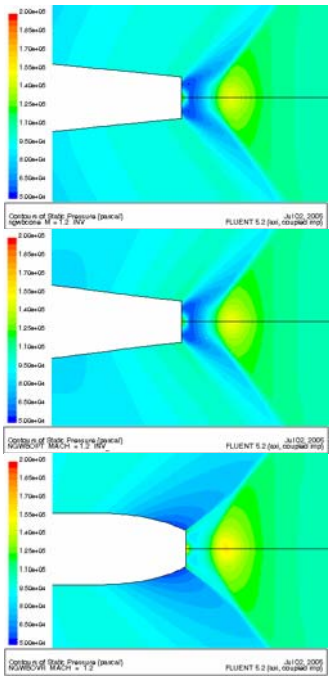

Fig. 6.14-a-b-c Static Pressure Contour of Case Study Geometry Body A, Body B and Body C (aft-body) for Mach = 1.2

Static pressure contour and velocity of the axi-symmetric slender body with base area under study are shown in Fig. 6.13-a-b-c to Fig. 6.15-a-b-c.

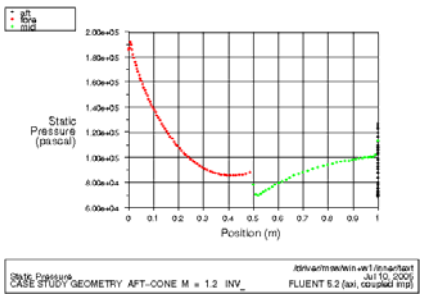

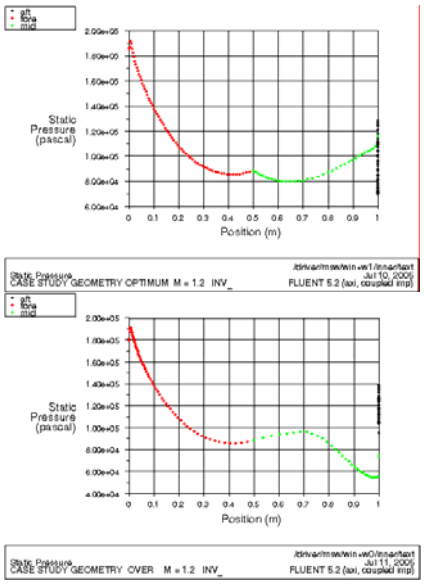

Fig. 6.15-a-b-c Static Pressure Distribution of Case Study Geometry Body A, Optimum, Over (aft-body) for Mach = 1.2

Figure 6.13-a-b-c shows the static pressure distribution around the body. Attached shock wave occurs at the nose for all geometries with the same fashion. It means that the fore body for all geometries gives the same contribution to the drag , and it is independent of shape of aft-body geometry. Weak expansion occurs at the starting point of aft-body curve for Body C and followed by a shock wave at wake downstream region. This pressure distribution will cause the very low pressure at base area region as depicted in figure 6.15-a-b-c. Therefore, the Body C has the highest drag compare with Body A and Body B.

7. Concluding Remarks

Three studies have been conducted. Analytical, numerical computation (CFD) and MFD optimization has been carried out to several axi-symmetric slender body configurations to search for geometry with minimum drag. In the first investigation, an analytical approach was used to look into the simplified transonic and supersonic gas dynamic equations following the work of Von Karman and Moore. This approach is conducted to the existing well-known axi-symmetric slender body, such as Sears-Haack, Von Karman and Haack-Adams geometry. This method is useful in estimating the characteristic of several axi-symmetrical slender body configurations.

In the second investigation, computational studies of the previous existing axi-symmetric slender body are

conducted to gain physical understanding of the effect of aft-body geometry to the overall wave drag. The CFD computations are made by using a commercially available flow solver Fluent/Rampant [21]. All of the CFD numerical approach is conducted for the condition of inviscid flow at Mach number 1.2 and 3.0, so only the pressure drag contributes to the total drag.

The CFD calculations have been conducted to the axi-symmetric slender body with pointed end as well as the axi-symmetric slender body with base area. For the axi-symmetric slender body with pointed end the results indicate that the weak expansion occurs on the shallow curve, while the strong expansion occurs on the steep curve. Usually, the strong expansion is followed by the appearance of strong shock waves on the aft body and weak expansion is followed by weak shock waves. The distribution of expansion and shock waves at the aft-body of the axi-symmetric slender body with pointed end alters the total drag. Modifying the contour of aft-body geometry will change the wave distribution and consequently alters the total drag. The optimum geometry is a body which has set of shock and expansion waves' distribution, in such a way that minimizes the wave drag.

For the axi-symmetric slender body with base, there are no shock waves generated on the aft body region on the axi-symmetric slender body with base area. Instead, expansion fans appear at the corners connecting the aft body to the base. The corner expansion fans turn the flow toward the centerline. As a result, a low pressure region occurs at the base area of the body. Also, the expansion fans deflect the flow coming from the upper and lower surfaces toward each other. Somewhere behind the base of the body, the two streams would meet and shock waves form near that location.

Based on the physical understanding gained above, a practical method of reducing the wave drag of a given body is developed for cases, body with pointed end and body with base area. In this method, a shock wave generator is placed at a particular location on the aft body. By trial and error, a particular location of the shock wave generator placement is found which result in lowering the wave drag. By CFD analysis, it is found that by placing the generator at this location, the aft body wave distribution induces a pressure distribution which lowers the wave drag of the body. The analysis indicates that there exists a particular shock wave generator location which results in generating an optimum aft body wave distribution and, hence, minimizes the wave drag of the body.

Finally, the third investigation is to find optimum geometries, which have minimum wave drag by utilizing Modified Feasible Direction (MFD) optimization program. The MFD optimization codes have been verified by evaluating a set of constraint that is consistent with Sears-Haack geometry and von Karman geometry. The optimization program is used to obtain the optimum aft-body of geometry of several case studies. Two geometries have been investigated: axi-symmetric slender body with pointed end and axi-symmetric slender body with base area. Both geometries consist of two parts, the fore-body and aft-body. The arbitrary fore-body is adopted from the MBB experimental body, for the case of body with pointed end. While the aft-body is formed by the polynomial of order three and the coefficient of the polynomial treated as the design variables. The aft-body for slender body with base consists of third order polynomial and has a base area with a radius of half of the maximum radius Using the specific set of constraints, the MFD program is used to find the optimum geometry which has minimum wave drag. In other words, in this approach the MFD program searches for an aft body geometry that generates an optimum wave distribution for minimizing the wave drag of the body. The results of this study show that the MFD optimization program provides a convenient way to solve an aerodynamic optimization problem which has not been done before.

References:

1. von Karman, T., The Problem of Resistance in Compressible Fluids, Proc.5th Volta Congress, Rome, pp.255-264, 1955.
2. von Karman, T., Compressibility Effects in Aerodynamics, J.Aeronaut.Sci., 8, pp.337-356, 1941. Fluids, Proc.5th Volta Congress, Rome, pp.255-264, 1955.
3. Sears, W.R.: On Projectiles of Minimum Wave Drag, Quarterly Appl.Math., vol. IV, no.4, Jan. 1947, pp. 361-366
4. Haack, W.: Geschossformen kleinsten Wellen-widerstandes, Lilienthal-Gesellschaft fuer Luftfahrtforschung, Bericht 130, Teil 1, October 9-10, 1941, pp.14-28; also Haack, W.: Projectile Shapes for Smallest Wave Drag, Translation No. A9-T-3, Contract W33-038-ac-15004 (16351), ATI No. 27736, Air Material Command, U.S.Air Force, Brown Univ., 1948.

5. Ward, G.N.: Supersonic Flow Past Slender Pointed Bodies, . Quart.Jour.Mech. and Appl.Math., Vol.II, pt.1, June 1949, pp.75-97.
6. Adams, M.C.: Determination of Shapes of Boattail Bodies of Revolution for Minimum Wave Drag. NACA TN 2550, 1951.
7. Parker, H.M., Minimum-Drag Ducted and Pointed Bodies of Revolution Based on Linearized Supersonic Theory. NACA Rep.1213, 1955.
8. Harder, K.C., and Rennemann, Jr., C., On Boattail Bodies Of Revolution Having Minimum Wave Drag, NACA Report 1271, Langley Aeronautical Laboratory, Langley Field, Va., June 8, 1955
9. Priyono, E. and Djojodihardjo, H., Computational Study Of The Aerodynamic Characteristics Of Axisymmetric Bodies In Transonic Flow, ICAS Paper 0375, 23rd ICAS Congress, Toronto, Canada, 2002.
10. Heaslet, M.A. and Fuller, F.B.: Axially Symmetric Shapes with Minimum Wave Drag, NACA Report 1256, 1955
11. Ashley, H and Landahl, M.T.: *Aerodynamics of Wings and Bodies*, Addison-Wesley Publishing Co,Inc., Reading, Massachussetts,USA., 1965.
12. Oswatitsch, K., and Keune, F., Ein Aequivalenzsatz fuer nichtangestellte Fluegel kleiner Spannweite in Scallnaher Stroemung, Z.Flugwiss., 3, No.2, 29-46, 1955.
13. Djojodihardjo, H and Widodo, A.F., Small Perturbation Computational Studies Of Two-Dimensional And Axisymmetric Slender Body In Transonic Flow, *The 3rd INDO- TAIWAN Workshop on Aeronautical Science and Technology*, Bandung, Indonesia, December 2002.
14. Djojodihardjo, H and Widodo, A.F.; Development Of A Simple And Fast Computational Routine To Solve The Full Potential Equation Of The Transonic Axi-Symmetric Flow, *Proc., 24th ICAS Congress, Yokohama, Japan August-September 2004*
15. Liepmann,H.W. and Roshko, A., Elements of Gasdynamics, Dover Publications, Inc., Mineola, New Yrk2001.
16. Vanderplaats, G.N. *Numerical Optimization Techniques for Engineering Design, with Applications.* McGraw-Hill Book Company, New York, 1984.
17. Vanderplaats, G.N., Efficient Algorithm for Numerical Airfoil Optimization, *AIAA Journal of Aircraft*, vol.16, no.12, pp.842-847, December 1979.
18. Lorenz-Meyer, W. and Aulehla, F. (1979) , *MBB – Body of Revolution No. 3* , AGARD AR 138, London.
19. Priyono, E. , Lavi R Zuhal and Djojodihardjo, H., *Numerical Study of Shock Generator at the Aft-Body of Slender Body of Revolution using Navier-Stokes Equation,* ICAS Paper 469, 24th ICAS Congress, Japan, 2004.
20. Prijono, E., *Optimization Of The Aft-Body Geometry Of An Axi-Symmetric Slender Body To Minimize Wave Drag, Doctoral Dissertation*, Departemen Teknik Penerbangan Institut Teknologi Bandung, October 2005.
21. Anonymous. *RAMPANT USER'S MANUAL*. Fluent Inc, Centerra Resource Park , Lebanon, NH 03766, June 1997.